To appear in the Proceedings of the SPIE Photonic East 95 - Mobile Robots X Conference, Philadelphia, Pennsylvania, October 1995.

Structured Light Systems for Dent Recognition: Lessons Learned

Juan C. Santamaría

College of Computing
Georgia Institute of Technology
Atlanta, Georgia 30332-0280 U.S.A.

Ronald C. Arkin

College of Computing
Georgia Institute of Technology
Atlanta, Georgia 30332-0280 U.S.A.

ABSTRACT

This paper describes the results from a feasibility analysis performed on two different structured light system designs and the image processing algorithms they require for dent detection and localization. The impact of each structured light system is analyzed in terms of their mechanical realization and the complexity of the image processing algorithms required for robust dent detection. The two design alternatives considered consist of projecting vertical or horizontal laser stripes on the drum surface. The first alternative produces straight lines in the image plane and requires scanning the drum surface horizontally, whereas the second alternative produces conic curves on the camera plane and requires scanning the drum surface vertically. That is, the first alternative favors image processing against mechanical realization while the second alternative favors mechanical realization against image processing. The results from simulated and real structured light systems are presented and their major advantages and disadvantages for dent detection are presented. The paper concludes with the lessons learned from experiments with real and simulated structured light system prototypes.

Keywords: structured light systems, dent detection, image processing.

1 INTRODUCTION

This paper describes the lessons learned on several hardware and software alternatives in the design of a structured light system[3,5] to detect dent and bumps (blisters) on drums. Savannah River Technology Center (SRTC) is developing the Stored Waste Autonomous Mobile Investigator (SWAMI-II) to provide inspection and survey of low-level nuclear waste drums. SWAMI-II will help insure the health and safety of workers by monitoring the condition of radioactive, hazardous waste. The SWAMI-II base vehicle is a modified version of the HelpMate mobile robot manufactured by Transitions Research Corporation (TRC). The vehicle will be equipped with a structured light system designed to recognize anomalies such as dents or blisters on a drum's surface. The drums are stored on pallets on both sides of each aisle. As the robot passes each drum, it will estimate the location of each drum to appropriately aim a structured light system, taking images of it with cameras mounted on the rear of the vehicle.

The objective of the dent recognition system is to detect dents and bumps (blisters) on a drum's surface. The requirements of the system are to be able to recognize dents greater than 1 inch (2.54 cm) laterally and vertically, and greater than 1 inch (2.54 cm) deep on the visible portion of each drum. The drums have a black, shiny surface and some paper labels and will be located on pallets on both sides of the robot. The basic design involves a laser and a camera. The laser projects a stripe on the drum's surface to make anomalies such as dents and blisters become visible as deformations of the laser stripe. Image processing software will analyze stored images off-board.

This paper describes the results from a feasibility analysis performed on two structured light system designs and the image processing algorithms they require for dent detection and localization. The two design alternatives considered consist of projecting either vertical or horizontal laser stripes on the drum surface. The first alternative produces straight lines in the image plane and requires scanning the drum surface horizontally, whereas the second alternative produces conic curves on the camera plane and requires scanning the drum surface vertically. That is, the first alternative favors image processing against mechanical realization while the second alternative favors mechanical realization against image processing.

In the general case, three different approaches for dent recognition were investigated. All of the approaches are variations on how to process an image of the drum surface illuminated by a laser beam. The first approach consists of zero-detection in the first derivative of the projected laser stripe. Points in which the first derivative evaluates to zero denote possible minima or maxima points on the laser stripe. These extreme points are candidate deformations on the drum's surface. The second approach consists of detecting outliers from a fitted model of the laser stripe. For example, all those points that lie beyond two standard deviations from the fitted model are candidate deformations on the drum's surface. The third approach involves spatio-temporal sampling to construct a 3-D model of the drum's surface.

This paper is organized as follows: Section 2 describes the structured light systems and their components as well as the image sampling techniques that are used to gather data. Section 3 describes the image processing algorithms for each of the three different approaches. Section 4 presents results using the alternatives based on images generated by both a simulation package and real-world laser striping prototypes. Section 5 presents an analysis of the results, a discussion of the advantages and disadvantages of each approach, and some recommendations for improving performance.

2 IMAGING HARDWARE

2.1 System design

SWAMI-II will be equipped with a mobile structured light system placed on the back of the vehicle. The structured light system will face toward a target drum at one side of the robot. As the robot navigates through the aisle, the structured light system will position itself, always pointing towards the center of the drum. Drums on the other side of the aisle will be scanned similarly during a second pass with the robot facing in the opposite direction.

Two structured light systems design were considered: horizontal scanning and vertical scanning. The former projects a vertical laser stripe on the drum surface while scanning the drum horizontally. The later projects a horizontal laser stripe on the drum surface while scanning the drum vertically. The horizontal scanning structured light system was the original design proposed by SRTC but was discarded afterwards due to the mechanical

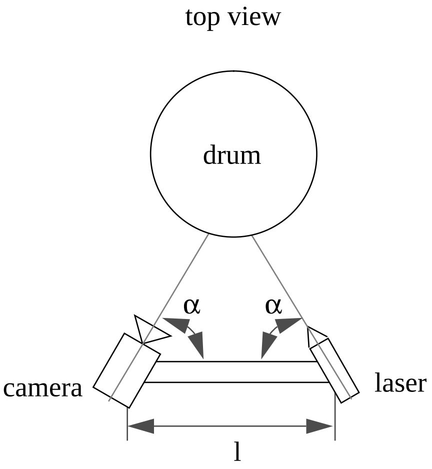

Figure 1: Horizontal scanning design

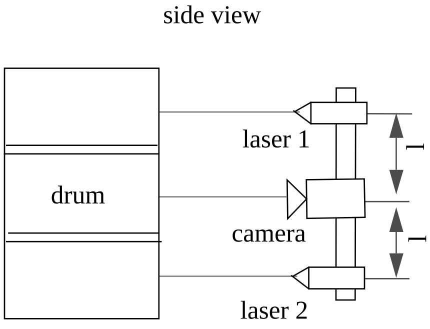

Figure 2: Vertical scanning design

complexity of its implementation.

The horizontal scanning structured light system design consisted of a laser and a camera mounted on a mobile platform. The camera and the laser were each fixed on the opposite extremes of a supporting bar arranged horizontally. The laser beam and the camera axis converge on a point located on an imaginary line perpendicular to the bar that crosses its midpoint. Figure 1 shows the horizontal scanning structured light system.

In the horizontal scanning design, as the robot navigates through an aisle, the structured light system moves in such a way as to always point to the center of the drum. The movement of the frame is performed by following the circumference keeping a constant distance between the structured light system and the surface of the drum. Figure 3 demonstrates this procedure. The laser projects an eye-safe beam that produces a laser stripe on the drum surface. Dents and bumps can be recognized by capturing and analyzing images containing this stripe.

The vertical scanning design consisted of two lasers and a camera mounted on a mobile platform. The two lasers are each fixed on opposite extremes of a supporting bar and the camera is located on the midpoint. The laser beams and the camera axis are parallel to each other and perpendicular to the drum surface. Figure 2 shows the redesigned structured light system.

Using this system, as the robot navigates through an aisle, it will stop at each drum, then the structured light system moves vertically to cover the drum surface. Figure 4 demonstrates this procedure. The lasers projects two eye-safe beams that will produce two laser stripes on the drum surface, one above and one below the center of the image. Dents and bumps can be recognized by capturing and analyzing images containing these stripes.

Image capture is the same in both designs. Images are captured at fixed intervals. Each image is thresholded and thinned in order to obtain a line description that occupies less space to store and is easier to process later on. Further details of the image processing depend on the particular approach selected. The next section describes each strategy in detail.

2.2 System components

The components used in the prototype systems are the same as the components specified for the current structured light system design. The following lists describes each component.

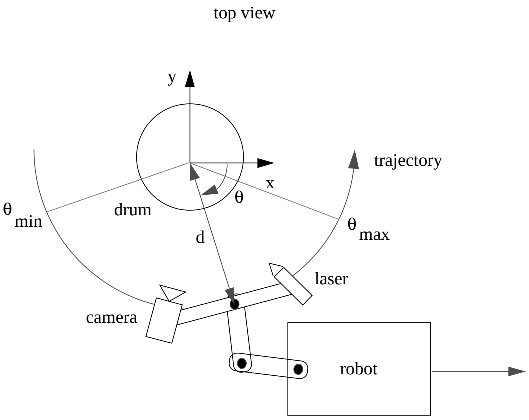

Figure 3: Sampling in the horizontal scanning design

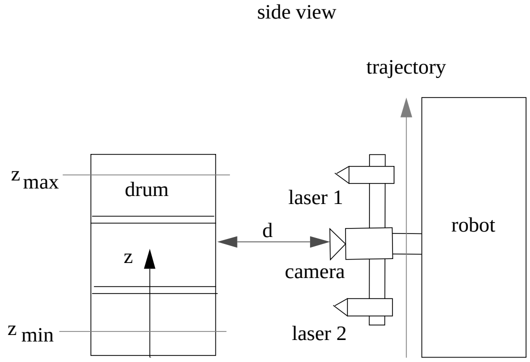

Figure 4: Sampling in the vertical scanning design

Camera: WATEC P/N WAT-203EX	Lens: JML P/N CTV 20080/100	Laser: Lasiris P/N SNF-501L-635M-3-45
CCD Size: 1/2” format 6.4 × 4.8 mm Horizontal Resolution: 550 TV Lines Sensitivity: 0.1 Lux Lens: C Mount External Sync (HD-VD) Size: 2.20″ × 2.44″ × 1.88″	Focal Length: 6.0 mm f/#: 1.2 Format: 1/2” CCD Mount: C Manual Iris Filter Diameter: M37.5 × 0.5 Length: 40 mm Diameter: 45 mm Weight: 110 grams	Wave Length: 635 nm @ 25 C° Power: 3 mW Class: IIa Stability: 0.25 nm/C° Fan angle: 45 degrees Modulation Option: Input TTL Frequency range: DC, 6 Hz – 2 MHz

3 VISUAL DENT DETECTION APPROACHES

This section describes in detail several approaches to detect dents on drum surfaces using either the horizontal or vertical scanning structured light system designs. Each approach uses a different image processing technique to detect possible deformations on the drum by analyzing the images captured with the structured light systems described in the previous section. All of the approaches utilize the same input formats and generate the same output. The differences involve the image processing technique used to detect the surface deformations.

There are two types of inputs to the dent detection software: configurational and data. The configurational input consists of information regarding the position and orientation of the laser and camera. The software only requires this information once at the beginning of execution. The data input consists of the images acquired by the camera. The software acquires this information periodically using it to detect and localize dents on drums. It is assumed that the structure supporting the laser and the camera always points toward the center of the drum while the structured light system scans the drum surface (refer to Figures 1 and 2). The input specifications follow:

1. **Frame Structure Information**. The following information is required for the configuration of the structured light system:
    (a) l: the distance in meters between the camera and the laser on the frame. Range: $[0, \infty)$
    (b) α: the angle in degrees between the longitudinal axis of the camera and the supporting frame. Range: $[0, 90]$

   (c) d: the distance between the middle point of the supporting frame and the center of the drum. Range: $[0, \infty)$

2. **Data Information**. The following information is required for each data sample:
   (a) $[I_n]$: the digitized image at that position. Range: I_n is an array of pixel values $[0, 255]$.

Ther output delivered by the dent recognition software consists of whether or not there is a dent in the processed image. The position of a detected dent can then be estimated considering the position of the structured light system at the time that image was taken.

3.1 Preprocessing algorithms and common image processing routines

The following image processing routines are general and most are used in both of the structured light system designs.

Cut: The purpose of this routine is to clip an image with a specified window and produce another image with only the information inside the given window. This function is required only in the vertical scanning structured light system and it is used to separate the top laser stripe from the bottom one. The window depends only on the configuration information and it is the same for each of the scanned images. In this way, each laser stripe can be processed individually and independently from each other.

Binarize: The purpose of this function is to contrast the pixels related to the laser beam from the background. The routine takes an image and a threshold value and produces a quantized two-valued image where all the pixels of the original with an intensity above the specified threshold are set to the maximum intensity value and the rest of the pixels are set to zero.

Average: The purpose of this routine is to produce a list of points (x, y) that represent the line produced by the projected laser beam on the image. **Average** scans the image column by column and returns the weighted row average of the for that column[1] (i.e. $y(x)$ is the center of mass across all rows at column x). Equation 1 shows the formula to estimate the row (y) for a given column (x).

$$y[x] = \begin{cases} 0 & \text{if } I_x = 0 \\ \displaystyle\sum_{r=0}^{r=R} r \frac{I(x, r)}{I_x} & \text{otherwise} \end{cases} \tag{1}$$

where $I_x = \sum_{r=0}^{R} I(x, r)$, and R is the total number of rows.

The result of this routine a thinned line that serves as the best estimator of the laser stripe projected on the drum surface. The thinned line is the basic input for all of the dent detection approaches.

Extrapolate: The purpose of this function is to fill up the empty spaces in a thinned line description of a laser stripe. Empty spaces are the result of low intensity spots in the laser stripe that were filtered out by the imaging or binarize operations. The interpolation is performed linearly using the two extreme points in the gap.

Smooth: The purpose of this function is to cancel out noise in a thinned line and produce a smoothed version of the laser stripe. The filter used is an unidimensional Gaussian kernel of a specified size S and bandwidth constant

---

[1] The direction of the scan depends on the orientation of the laser stripe. Horizontal laser stripes are scanned column by column and vertical laser stripes are scanned row by row.

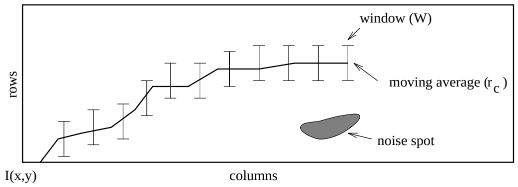

Figure 5: Moving-window-average

B. Equation 2 shows the formula to calculate the smoothed y for each x.

$$y[x] = \sum_{t=-S/2}^{S/2} y'[x-t]\text{Gaussian}[t] \tag{2}$$

where $y'[\cdot]$ is the periodic expansion of $y[\cdot]$ and $\text{Gaussian}[t] = \exp(-\frac{t^2}{B})$ is the filter that spans from $-S/2$ to $S/2$.

Moving-Window-Average: Similar to **Average**, the purpose of this routine is to produce a list of points (x, y) that represent the line produced by projected laser beam on the image. The difference is that the **Moving-Window-Average** routine estimates the y coordinate of each point by calculating a weighted average over a small window centered on the moving average of the last N points. In this way, bright spots that are produced by reflection or refraction of the laser beam are filtered out. Figure 3.1 shows the procedure and Equation 3 shows the formula used to estimate the row (y) given column (x). This function was created to overcome noisy bright spots on the images taken with the prototype system in the real world.

Moving-window-average is computed using:

$$y[x] = \begin{cases} 0 & \text{if } I_x = 0 \\ \displaystyle\sum_{r=r_c-W/2}^{r_c+W/2} r\frac{I(x,r)}{I_x} & \text{otherwise} \end{cases} \tag{3}$$

where $I_x = \displaystyle\sum_{r=r_c-W/2}^{r_c+W/2} I(x,r)$, which is the center of mass across W rows at column x and centered at row r_c, and r_c is the moving average of the last N points, which is updated for the following column using the following an exponential smoothing formula: $r_c \leftarrow \frac{N}{N+1}r_c + \frac{1}{N+1}y[x]$.

3.2 Dent detection approaches using vertical laser stripes

This section describes two approaches used to detect dents on drum surfaces. Vertical laser stripes result from the horizontal scanning structured light system design. The approaches described here take advantage of the projection of vertical laser stripes over cylindrical surfaces. This simplifies the task of detecting dents because a vertical laser stripe projected over a smooth cylindrical surface produces a vertical line in the image plane. Thus, any deviations from a vertical line are an indication of the presence of an anomaly on the surface.

First Derivative Approach:

One way to detect deformations on the drum's surface consists of detecting the maxima and minima points

```
For every captured image $I(x,y)$:
1.   Binarize the image.
2.   Average binary image to produce thinned line.
3.   Smooth thinned line with a Gaussian filter.
4.   Calculate the first derivative.
5.   Detect all the points that evaluate to zero.
6.   Report a list of all the maxima and minima points above limits.
```

Figure 6: Zero Detection Algorithm.

```
For every captured image $I(x,y)$:
1.   Binarize the image.
2.   Calculate column sample mean $\bar{x}$ and sample column standard deviation $\sqrt{s^2}$
3.   Detect all outlying points $I_{\text{binary}}(x,y) = 1$ such that $|y - \bar{x}| > k\sqrt{s^2}$
4.   Report a list of all the consecutive outlying points above a limit.
```

Figure 7: Outliers Detection Algorithm.

of the projected laser stripe in the captured image. Minima and maxima points are candidates for estimating the size of the deformations on the drum's surface. A maximum or a minimum point of a function can be detected by analyzing the first derivative of such a function and detecting the points in which it evaluates to zero. Maxima and minima points are points in which the first derivative is zero. Then, the magnitude of the deviation from the straight line to the extreme point can be used to estimate the deformation on the drum surface.

Before estimating the first derivative of the laser stripe in an image, some preprocessing is required. First, the image must be thresholded to discard all information not related to the portion of the drum where the laser is projected (i.e., apply **Binarize**). Second, all the horizontal points of the stripes are averaged together to produce a single point per row (i.e., apply **Average**). In this way, the original vertical laser stripe is condensed to a vertical line. Third, the line is smoothed with a Gaussian kernel to filter out noise (i.e., apply **Smooth**). Finally, the first derivative is estimated and the zero crossing points are detected. One last step verifies the magnitude of the maximum and minimum points to detect valid dents and blisters on the drum surface. The algorithm is shown in Figure 6.

Outliers Approach:

As in the previous approach, the purpose of this approach is to detect deformations on the drum's surface by detecting deviations of the projected laser stripe. However, instead of finding the maximum and minimum points on a preprocessed vertical line, this method concentrates on locating points that are far from the vertical stripe in a statistical sense.

The best line fit to the projected laser stripe can be calculated using least squared estimation (LSE).[2] Then, all the outlying points can be identified and the dents detected if there exist enough consecutive outlying points. For the simple case of a vertical straight stripe, the mean and the standard deviation of all the points in the thresholded image are calculated. Then, all of the points lying beyond some constant multiple of the sample standard deviation ($\sqrt{s^2}$)are reported as outliers. The algorithm is shown in Figure 7.

---

[2] In this case, the LSE of the best vertical line is simply the sample average (i.e., $x = \bar{x}$).

```
For every captured image $I(x,y)$:
1.   Cut the image into top and bottom sections.
2.   Calculate thinned lines using the Moving-Window-Average routine.
3.   Smooth thinned lines with a Gaussian filter.
4.   Calculate the second derivative.
5.   Detect all outlying points.
6.   Report a list of all the outlying points above limits.
```

Figure 8: Second-derivative Algorithm.

3.3 Dent detection approaches using horizontal laser stripes

This section describes three approaches used to detect dents on drum surfaces. Horizontal laser stripes result from the vertical scanning design of the structured light system. Projecting horizontal laser stripes over cylindrical surfaces produces a curved line on the image plane of the camera (i.e., a conic). Detecting dents is not as simple as when analyzing vertical stripes because the reference is not a linear function.

Using a simple camera model[1] it can be shown that the laser stripe is projected on the image plane as a section of an ellipse. However, given the current structured light system design and the field of view of the lens, the camera can cover at most 1/3 of the drum surface.[3] Under this configuration, the section of the ellipse can be approximated by a parabola without significant error. The approaches described here take advantage of a parabolic model of the line in the image plane. Thus, any deviations from this model can be considered as an indication of an anomaly on the surface on the drum.

Deviations from Second Derivative Approach:

Since the reference model is a parabola, a simple way to detect deformations on the drum's surface consists of detecting when the quadratic coefficient is not constant. That is, taking the second derivative of the line and detecting outliers from its mean. Outlying points only provide information about strong deviations from the reference model (i.e., a parabola). In order to estimate the magnitude of the deformation on the drum surface it is necessary to calculate the best fitting parabola and consider the difference between the parabola and the line, both evaluated at the outlying points.

Before estimating the second derivative of the laser stripe in an image, some preprocessing is required. First, the image is clipped to produce two image sections: one with the top laser stripe and the other with the bottom laser stripe. Second, each of the image sections is preprocessed with the **Moving-Window-Average** routine described previously to produce thinned lines. Third, the lines are smoothed with a Gaussian kernel to filter out noise. Finally, the second derivative is estimated and the outlying points are detected. One last step verifies the magnitude of the outlying points to detect valid dents and blisters on the drum surface. The algorithm is shown in Figure 8.

Outliers from a Fitted Parabola:

As in the previous approach, the purpose of this approach is to detect deformations on the drum's surface by detecting deviations of the projected laser stripe from its reference model. However, instead of calculating outliers relative to the second derivative, this method concentrates on fitting the best parabola to the given points and detecting outliers from the fitted curve in a statistical sense.

The LSE estimation of the best fitting parabola to the projected laser stripe is calculated using the list of

---

[3] For this reason the structured light system consists of three cameras and six lasers. Each camera and its respective pair of lasers cover 1/3 of the total surface of the drum.

```
For every captured image $I(x,y)$:
1.   Cut the image into top and bottom sections.
2.   Calculate thinned lines using the Moving-Window-Average routine.
3.   Estimate parameters of the polynomium $p(x) = \beta_0 + \beta_1 x + \beta_2 x^2$
4.   Detect all outlying points such that $|y(x_h) - p(x_h)| > k\sqrt{s^2_{x_h}}$
     where $\sqrt{s^2_{x_h}} = \mathbf{X_h}^T(s^2\mathbf{X}^T\mathbf{X}^{-1})\mathbf{X_h}$
5.   Report a list of all the consecutive outlying points above a limit.
```

Figure 9: Parabolic Model Outliers Detection Algorithm.

points (x, y) from the thinned line.[2] Then, all the outlying points are identified and dents reported as detected if there exist enough consecutive outlying points. For the case of a parabola (i.e., a second order polynomium), the sample standard deviation of a point depends on its offset from the mean and the inherent error in the signal. All the points beyond some constant of its sample standard deviation can be reported as outlying. The algorithm is shown in Figure 9.

The LSE estimation of the parameters is based on a model is of the form:

$$Y_i = \beta_0 + \beta_1 X_i + \beta_2 X_i^2 + \epsilon_i$$

where $i = 1, \ldots, n$ and n is the number of points.

The previous equation can be compactly written in matrix terms as follows:

$$\boldsymbol{Y} = \boldsymbol{X\beta} + \boldsymbol{\epsilon}$$

where $\mathbf{Y} = \begin{bmatrix} y_1 \\ \vdots \\ y_n \end{bmatrix}$, $\mathbf{X} = \begin{bmatrix} 1 & x_1 & x_1^2 \\ \vdots & \vdots & \vdots \\ 1 & x_n & x_n^2 \end{bmatrix}$, $\boldsymbol{\beta} = \begin{bmatrix} \beta_0 \\ \beta_1 \\ \beta_2 \end{bmatrix}$, and $\boldsymbol{\epsilon} = \begin{bmatrix} \epsilon_1 \\ \vdots \\ \epsilon_n \end{bmatrix}$.

Given the above formulae, the least squared error estimation of $\boldsymbol{\beta}$ can be calculated as:

$$\hat{\boldsymbol{\beta}} = (\mathbf{X}^T\mathbf{X})^{-1}\mathbf{X}^T\mathbf{Y}$$

It is important to mention that the previous formulae estimate the parabola that minimizes the cost function $Q = \sum_{k=1}^{n}(y_k - \hat{y_k})$. However, if there is a relatively small rotation between the drum and the image plane of the camera as depicted in Figure 10, then it is required to find at which image plane angle the cost function $Q(\cdot)$ is minimized. The algorithm in Figure 11 uses gradient descent to find the best fitting parabola when the frame of reference is allowed to rotate freely (i.e., finds the LSE estimation of the best fitting parabola assuming there is a misalignment with the axis of the drum and the normal vector of the image plane).

Spatio-Temporal Approaches:

This approach uses each projected laser stripe to progressively construct a 3-D model of the drum's surface.[4] This 3-D model is then analyzed to detect dents of different sizes and shapes. Constructing a 3-D model is possible by fitting a parabola to consecutive curves and using it as a reference. With this information, it is possible to estimate the depth of each point on the drum surface given the deviation of its corresponding point on the reference surface. Thus, by combining the information of the points of the laser stripes of images captured at different positions, a three dimensional grid of the drum's surface can be estimated. Such a grid can then be processed to locate and detect dents and blisters of arbitrary shape.

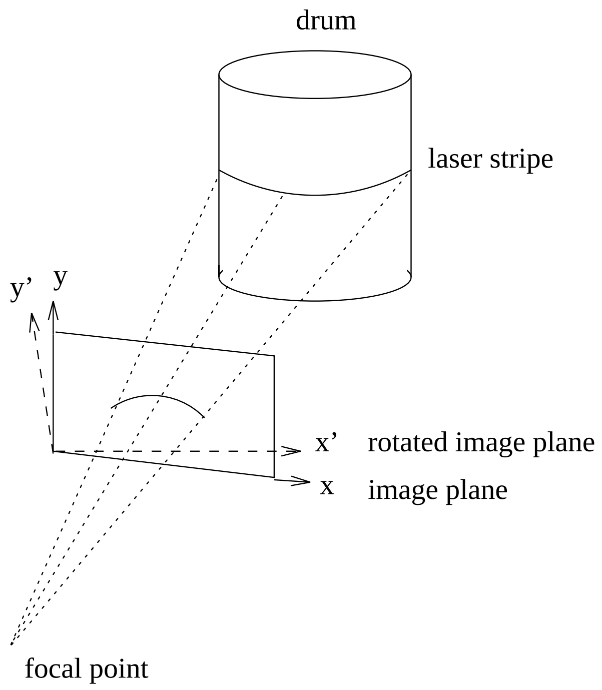

Figure 10: Camera model with rotated image plane.

```
For a thinned line description $(x_i, y_i)$ and $i = 1, \ldots, n$:
1.   Standardize all points:  $(x_i, y_i) \rightarrow (x'_i, y'_i)$
     where $x'_i = (x_i - \bar{x})/\sqrt{s_x^2}$ and $y'_i = (y_i - \bar{y})/\sqrt{s_y^2}$
2.   $l \leftarrow$ min_angle, $r \leftarrow$ max_angle.
3.   while $(r - l < \epsilon)$
       3.1.  $m \leftarrow \frac{l+r}{2}$
       3.2.  Rotate all points an angle $m$
             $\begin{bmatrix} x_{r_i} \\ y_{r_i} \end{bmatrix} = \begin{bmatrix} \cos(m) & \sin(m) \\ -\sin(m) & \cos(m) \end{bmatrix} \begin{bmatrix} x'_i \\ y'_i \end{bmatrix}$
       3.3.  Estimate best parabola $(x_{r_i}, fy_{r_i})$ for $(x_{r_i}, y_{r_i})$
       3.4.  Calculate cost:  $Q \leftarrow \sum_{k=1}^{n} (y_{r_i} - fy_{r_i})^2$
       3.5.  If $\frac{\partial Q}{\partial m} = 0$ exit
       3.6.  If $\frac{\partial Q}{\partial m} > 0$ $r \leftarrow m$
       3.7.  If $\frac{\partial Q}{\partial m} < 0$ $l \leftarrow m$
```

Figure 11: Rotated Regression Algorithm.

```
1.   For all the images $I_n(x, y)$ of a drum:
      1.1.   Cut the image into top and bottom sections.
      1.2.   Calculate thinned lines using the Moving-Window-Average routine.
      1.3.   Smooth thinned lines with a Gaussian filter.
      1.4.   Estimate reference curve using the $k$ consecutive smoothed lines.
      1.5.   Construct three-dimensional grid by subtracting thinned lines and the reference curves.
2.   Scan three-dimensional grid for dents and blisters.
3.   Report a list of all the dents and blisters.
```

Figure 12: 3D Modeling Algorithm.

As in the previous approaches, some preprocessing of the raw image is required to reduce the amount of noise. The preprocessing steps involve estimating the thinned line using the moving window average routine, extrapolating missing points, and smoothing the resultant curve with a Gaussian filter. The algorithm is shown in Figure 12.

4 RESULTS

Experiments with the horizontal scanning structured light system were performed in simulation only because the mechanical realization of a prototype proved too expensive. Experiments with the vertical scanning structured light system were performed with two prototypes: one was assembled at the Georgia Tech Mobile Robot Laboratory (GT-prototype) and the other one was assembled by Savannah River Technology Center personnel (SRTC-prototype). Figures 21a and 21b show a picture of the prototypes. Both prototypes have the camera rotated 90 degrees clockwise to take advantage of greater resolution in the horizontal axis of the image plane. This also means that horizontal lines on the drum surface look vertical on the image. The following subsections present the results of the preprocessing routines, the horizontal, and vertical scanning structured light systems.

4.1 Preprocessing Routines

All the figures presented here are based on image series taken with the SRTC-prototype.

Cut: This routine takes a portion of an image. Figure 13 shows a 512×486 image and the result of a **Cut** operation with window starting at $(95, 0)$, 35 columns wide and 486 rows tall (center). The bright spots results from specular reflections produce by the camera's lens and the shiny drum surface.

Binarize: This routine creates a binary image. Figure 13 shows a 35×486 image (center) and the result of a **Binarize** operation with threshold 20 (right).

Average: This routine creates a thinned line from an image. Figure 14 the result of an **Average** operation to the 35×486 image from Figure 13 (center).

Smooth: This routine filters noise from a thinned line. Figure 15 shows the result of a **Smooth** operation of size of 43 pixels and bandwidth constant of 7 pixels applied to the thinned line in Figure 14.

Moving-Window-Average: This routine creates a thinned line from an image. Figure 16 shows the result of a **Moving-Window-Average** operation with window 10 to the 35×486 image from Figure 13 (center).

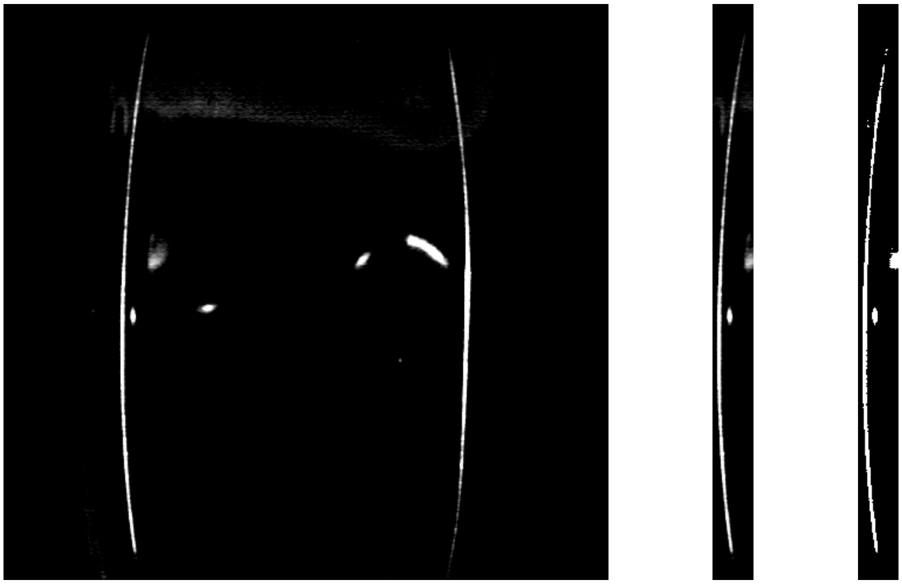

Figure 13: Left: the original image. Center: its bottom portion. Right: binarized.

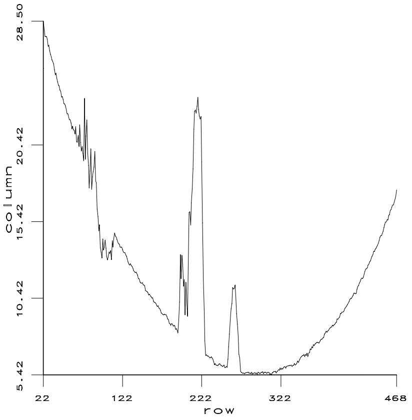

Figure 14: Thinned line.

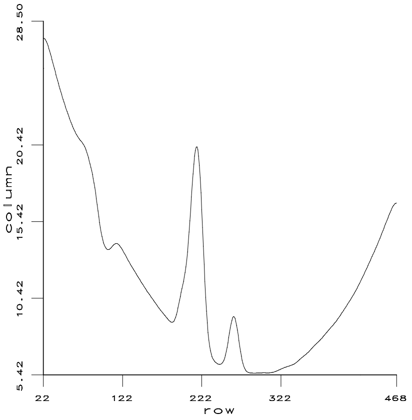

Figure 15: Smoothed line.

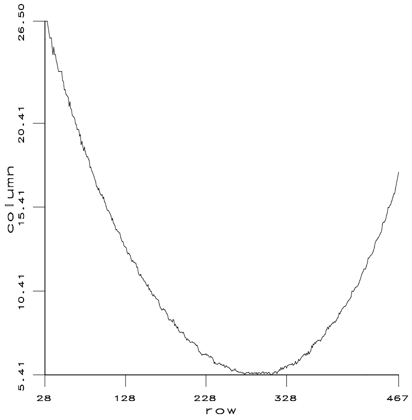

Figure 16: Moving-Window-Average thinned line.

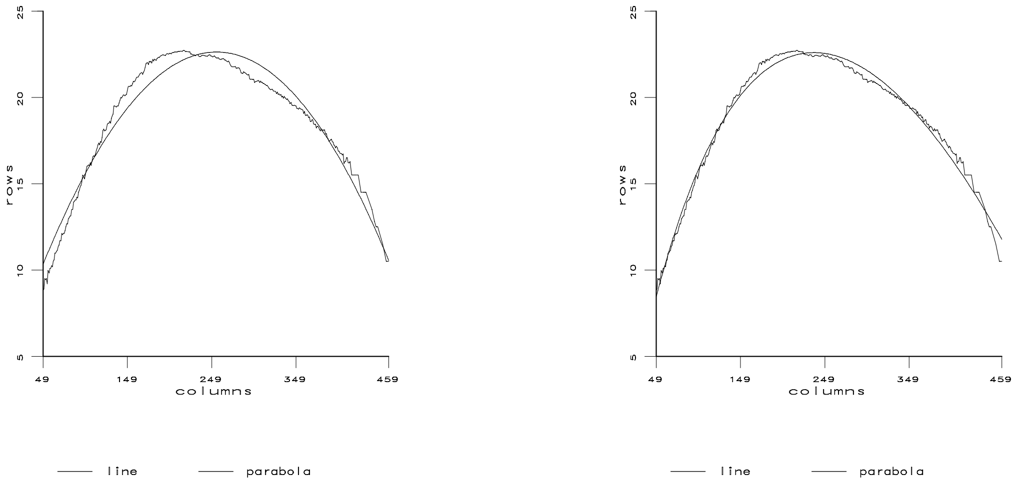

Figure 17: Left: Standard regression. Right: Regression with rotation.

Regression: Although this is not a preprocessing routine, an example of the difference between the standard regression and the algorithm in Figure 11 is shown below. Figure 17 shows the fitted parabola to a thinned line.

4.2 Horizontal scanning structured light system

All the experiments performed on the horizontal scanning structured light system were simulated. All images were generated using the RAYSHADE environment. The simulated structured light system has the following parameters (refer to Figures 1 and 3): $l = 10\text{cm}$, $\alpha = 81^\circ$, $d = 80\text{cm}$, and $-150^\circ \leq \theta \leq -30^\circ$. Images were captured every 5 degrees. The model of the drum contained three dents and three bumps. Figure 18 shows the model of the drum used during these experiments.

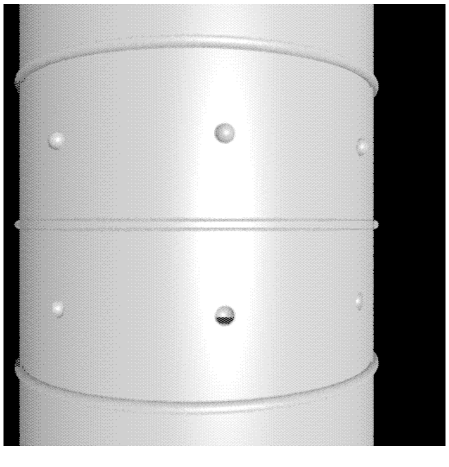

Figure 18: Drum Model.

First derivative approach: Figure 19 shows the different steps of the zero-detection algorithm of the image at position $\theta = -135°$.

Outliers approach: Figure 20 shows the different steps of the outlier-detection algorithm of the image at position $\theta = -135°$.

4.3 Vertical scanning structured light system

The GT-prototype and the SRTC-prototype were used to perform experiments using the current structured light system design. The GT-prototype consists of one camera and one laser mounted 4.5 inches above the camera. Figure 21 a shows a picture of the prototype. The SRTC-prototype was designed and developed at the Savannah River Technology Center. The SRTC-prototype consists of one camera and two lasers. Figure 21b shows a picture of the prototypes.

Deviations in Second Derivative Approach: Figure 22 shows the results for different steps of the second derivative algorithm. The image was gathered using the GT-prototype. There is one dent of depth 1/8 of an inch (approx.) in the center.

Outliers from fitted parabola: Figure 23 shows the different steps of the algorithm that detects outliers from the best fitted parabola. The image was gathered using the GT-prototype. There is one dent of depth 1/8 of an inch (approx.) in the center.

Spatio-Temporal Approach: Figure 24 shows the different steps of the spatio-temporal algorithm. Images were gathered using the SRTC-prototype. The processing was performed using 17 images, each one is taken by vertically moving the light system 50 mils down (i.e., vertical scanning every 50 mils). The top portion of the images cover a total of 5 artificial created bumps (three to the right and two to the left).

5 DISCUSSION AND RECOMMENDATIONS

In general, all the approaches presented here can be used to detect dents on drums. However, some approaches are more sensitive to noise and lighting conditions. Approaches that are based on derivatives are very sensitive to noise, but smoothing operations can reduce the variability. There is a compromise between strong filtering to reduce the noise and the desired resolution for dent detection. The more the filter rejects noise the less chance of detecting small dents.

Specular reflection is a major problem for line extraction because the images contain spots of bright light near the lines (see right of Figure 13). These bright spots tend to bend the line during the thinning operation, which can trigger the dent detection algorithm and produce false positives. The **Moving-Window-Average** routine can help solve this potential problem effectively as shown in Figure 16.

Positioning and misalignment are another source of errors. Figure 17 shows the systematic error that can be introduced by fitting a parabola assuming perfect alignment between the axis of the drum and the image plane. The reason for this is that the regression equations minimize the squared difference in the ordinates axis only. The algorithm in Figure 11 corrects this problem by searching the rotation angle that minimize the squared difference in the ordinate axis.

One major problem with the structured light system is the ambient lighting conditions. The experiments performed at Georgia Tech and in Savannah River Laboratories were performed under rigorous lighting constraints.

Figure 19: Zero detection images. Top left is the raw image. Top right is the thresholded image. Middle left is the mean of rows. Middle right is the smoothed line (expanded). Bottom is the first derivative (expanded). The two bumps were detected (plus two ribs).

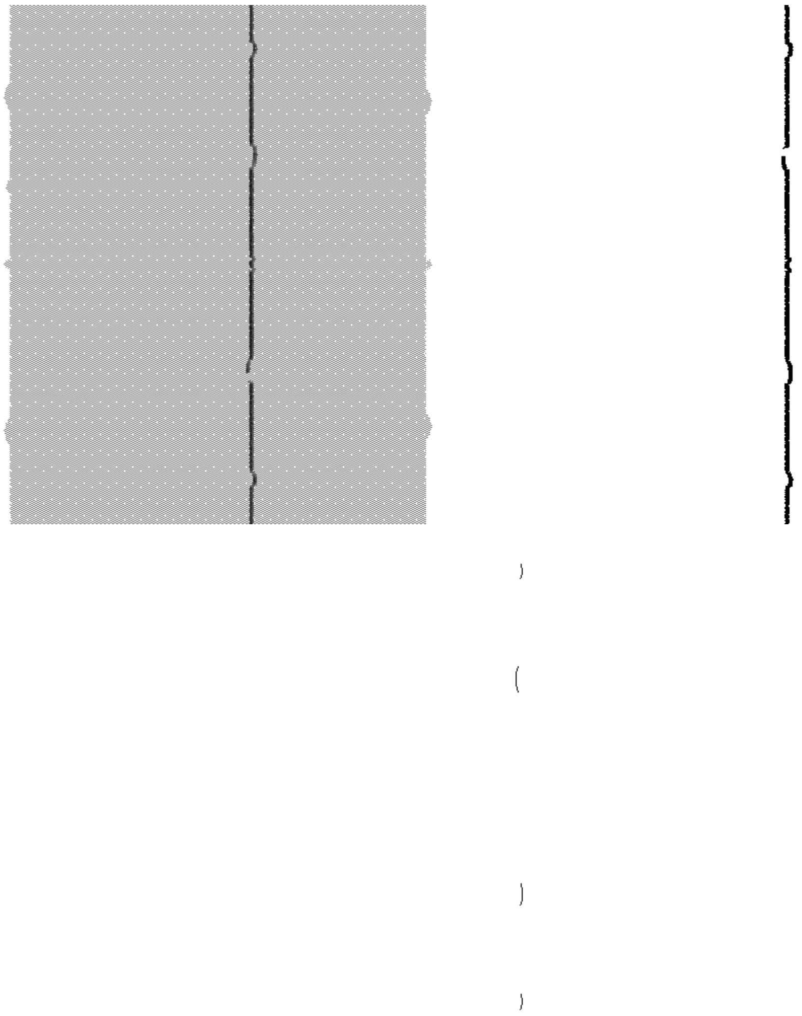

Figure 20: Outliers images. Top left is the raw image. Top right is the thresholded image. Bottom shows outliers ($k = 2$). Two two bumps were detected (plus two ribs).

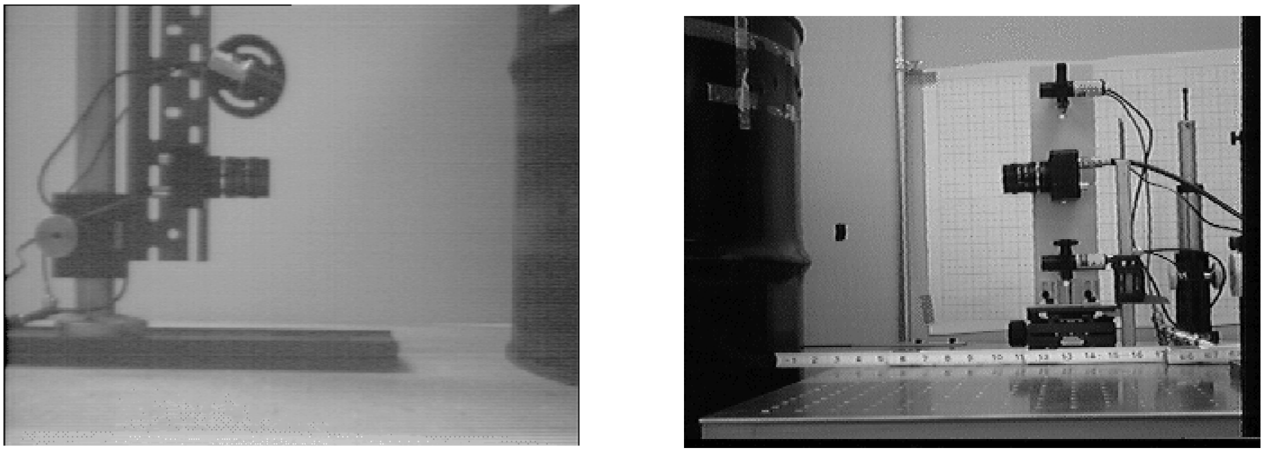

Figure 21: Prototypes: GT-prototype (left) and SRTC-prototype (right).

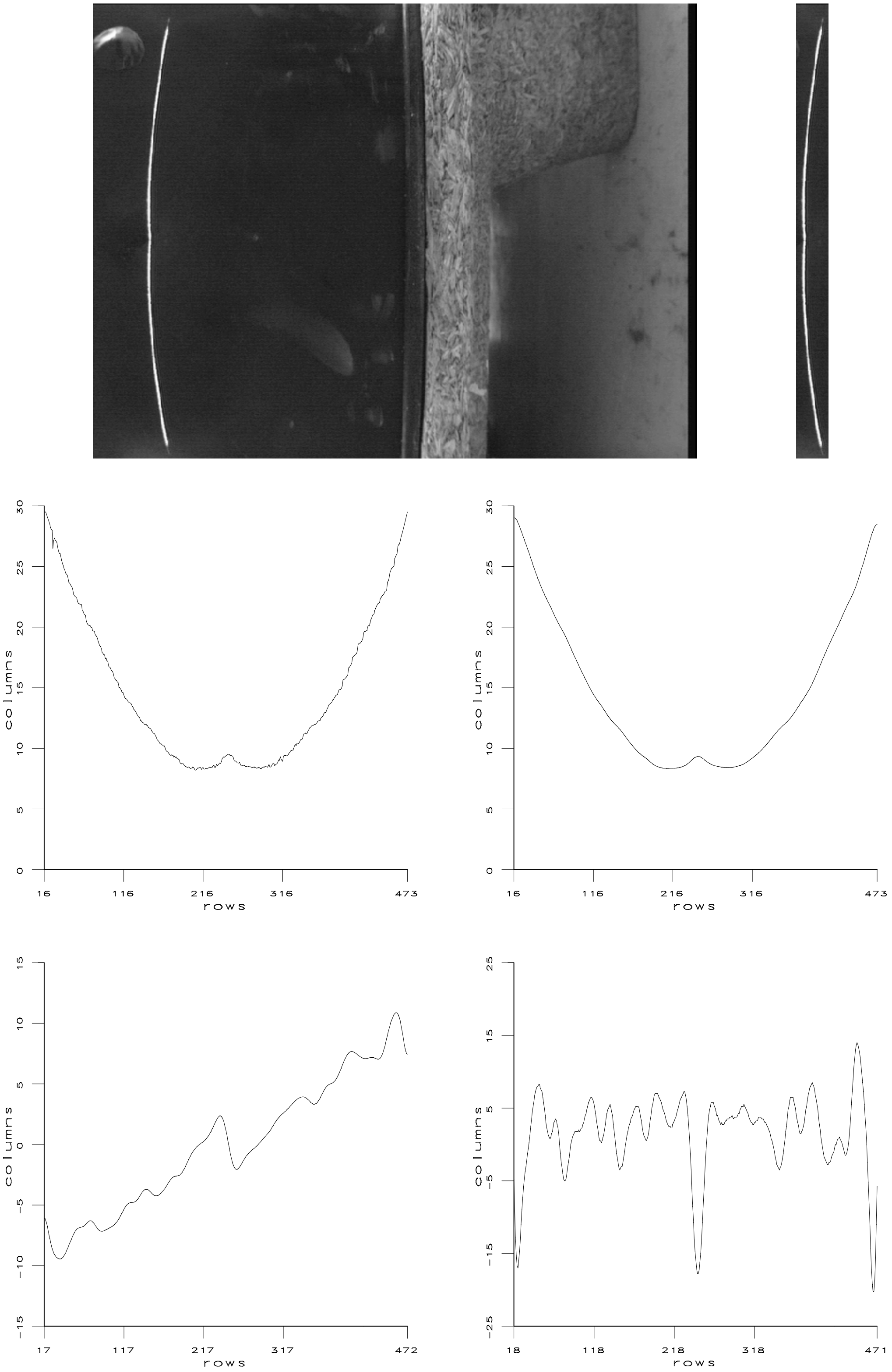

Figure 22: Deviations in second derivative. Top left is the raw image. Top right is relevant portion. Middle left is the thinned line. Middle right is the smoothed line. Bottom left is the first derivative. Bottom right is the second derivative. The dent is readily detected.

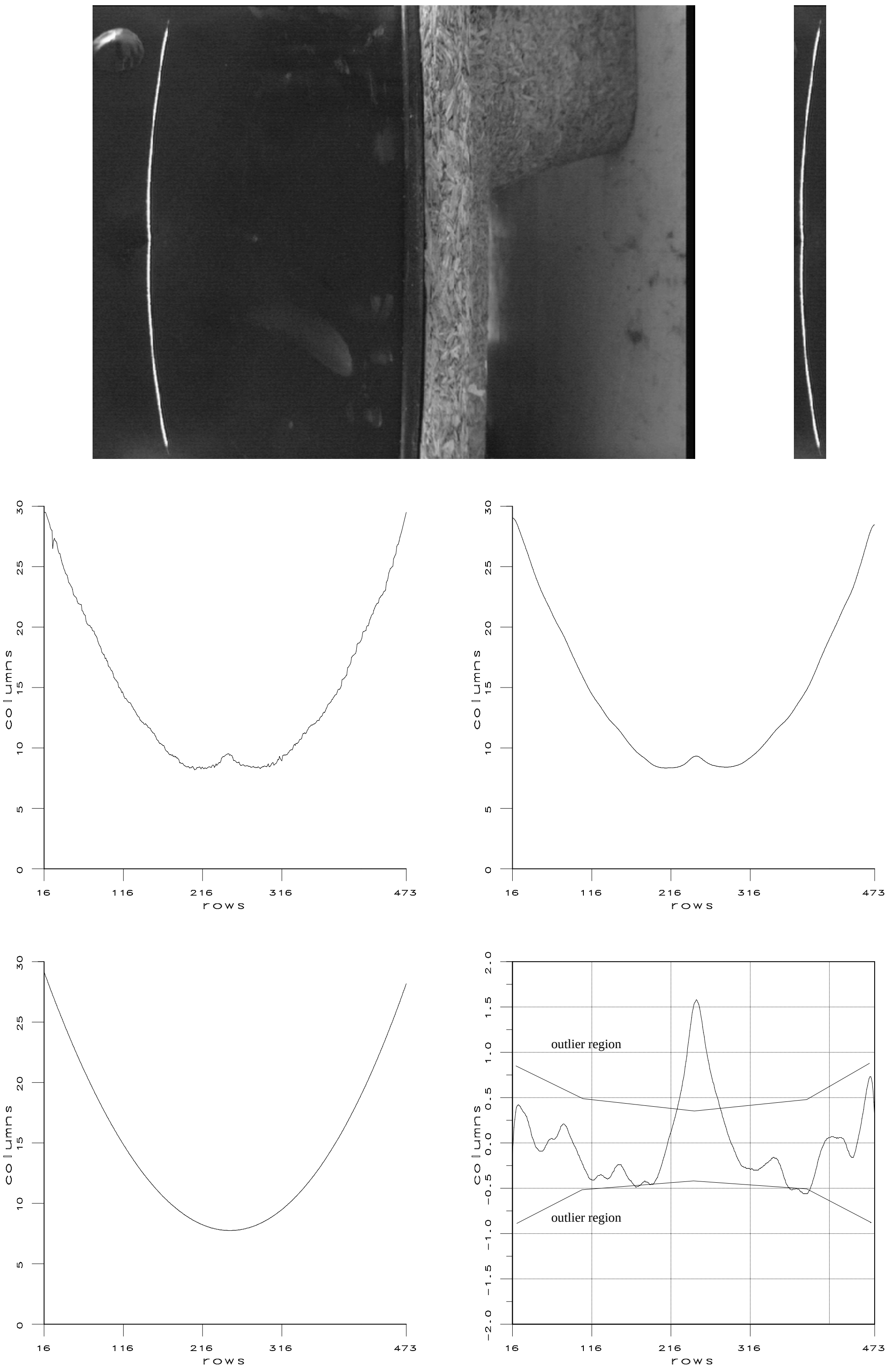

Figure 23: Outliers from fitted parabola. Top left is the raw image. Top right is relevant portion. Middle left is the thinned line. Middle right is the smoothed line. Bottom left is the fitted parabola. Bottom right is the difference between the smoothed line and the parabola showing the outlying regions. The dent is readily detected.

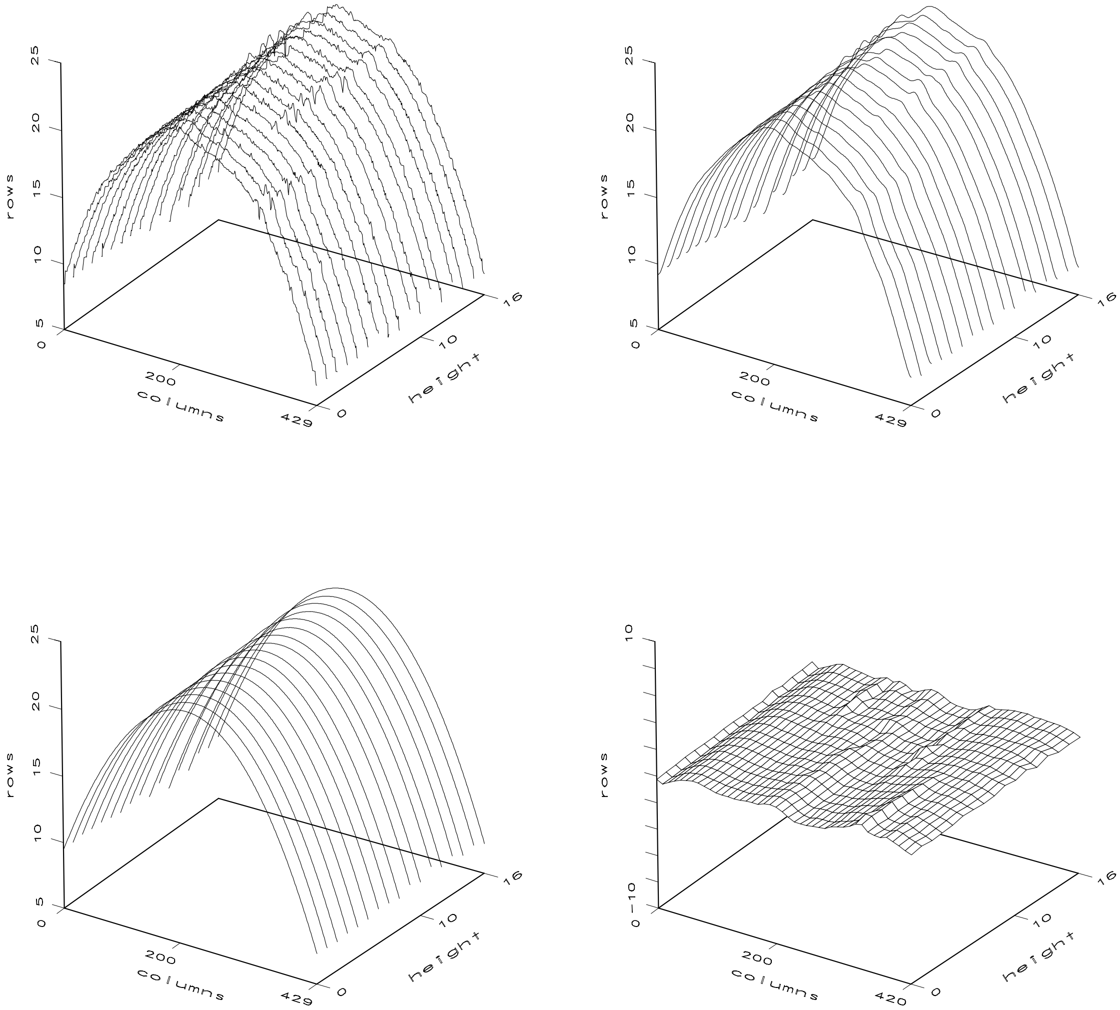

Figure 24: Spatio-temporal approach. Top left is the set of original thinned lines. Top right is the set of smoothed lines. Bottom left is the set of fitted parabolas. Bottom right is the difference between the smoothed lines and the parabolas.

However, none of the two prototype systems used included a red filter to enhance laser strip contrast and reduce ambient light. It is expected that a red filter can assist in solving this problem, but further evaluation is necessary.

The sensitivity of the vertical scanning structured light system design is too low considering the amount of noise and size of the dents. Considering some images taken from the SRTC-prototype, there is a difference between the closest point (center of image) and the farthest point (one of the sides) of 20 pixels. 55-gallon drums, have a radius of 12 inches approximately. Since the camera covers 1/3 of half the drum surface, the sensitivity of the structured light system is about 0.3 inches/pixels.

In the vertical scanning structured light system design, the axis of camera and the laser light plane are parallel. The focal length and the distance between the lens and the drum are the two parameters that determine the sensitivity of the system. Reducing the distance between the drum and the camera or increasing the focal length will increase the sensitivity. However, both alternatives reduce the field of view of the camera. A third alternative consists of projecting the lasers at an angle. This can increase the deformation of the line on irregular surfaces and indirectly increase the sensitivity of the system.

6 ACKNOWLEDGMENTS

This research was supported by the Westinghouse-Savannah River Technology Center. Additional funding for the Mobile Robotics Laboratory is provided by ARPA/ONR, the U.S. Army Applied Aviation Directorate, and the NAtional Science Foundation.

7 REFERENCES

[1] R.O. Duda and P.E. Hart. *Pattern Classification and Scene Analysis*, Chapter 7, Wiley, New York, 1973.

[2] J. Neter, W. Wasserman, and M.H. Kutner. *Applied Regression Models*, Chapters 6 and 9, Prentice Hall, New Jersey, 1989.

[3] D. Lake. "Lighting and Imaging, Part 2: Making it All Work Right," *Advanced Imaging*, pp. 66–89, June, 1994.

[4] A.C. Kak. "Depth Perception For Robots", *Handbook of Industrial Robotics*, Shimon Y. Nof (ed.), pp. 272–319, John Wiley & Sons, New York, 1985.

[5] D. Wei and M. Gini. "The Use of Taper Light Beam for Object Recognition," *Robot Vision*.

[6] W.J. Wolfe, J. Gunderson, and M.E. Walworth. "Computer Vision Barrel Inspection," *SPIE Mobile Robots VIII*, Vol. 2058, pp. 128–133, 1993.